Magnetoplasmons in a Tunable Periodically Modulated Magnetic Field

S. Cinà,[1,2] D. M. Whittaker,[2] D. D. Arnone,[2] T. Burke,[1] H. P. Hughes,[1]
M. Leadbeater,[2] M. Pepper,[1,2] and D. A. Ritchie[1]
[1]*Cavendish Laboratory, University of Cambridge, Madingley Road, Cambridge, CB3 0HE United Kingdom*
[2]*Toshiba Research Europe Limited, 260 Cambridge Science Park, Cambridge, CB4 0WE United Kingdom*
(Received 2 June 1999)

We report the first infrared optical measurements of a two dimensional electron gas (2DEG) in a periodically modulated magnetic field. The 2DEG is produced using epitaxial regrowth on a corrugated surface, so that the component of an externally applied magnetic field perpendicular to the 2DEG is spatially modulated. Two active modes are observed, with intensities and frequencies which depend on the amplitude of the field modulation as well as the total external magnetic field. These modes arise from field modulation-induced coupling between the 2DEG magnetoplasmons. Calculations of the magnetoplasmon band structure in a modulated field are in excellent agreement with the experimental data.

PACS numbers: 78.66.–w, 73.20.At, 73.20.Mf

Band structure effects arising from periodic modulations can be observed in a wide range of a physical systems. Electron energy bands produced by the periodic potential in a crystal, photonic band structures in systems with periodic dielectric constants, and plasmons in charge density modulated systems, are just some examples of systems in which mode dispersions show energy gaps at the edges of the Brillouin zone due to a periodic modulation. The effects of periodic electrostatic potentials on a two dimensional electron gas (2DEG) have been extensively studied theoretically and experimentally [1], and there is now increasing interest [2–12] in the effects produced by a novel form of periodic potential—that produced by a periodically modulated magnetic field (PMMF).

PMMF investigations to date have been largely theoretical. It has been predicted that the sharp Landau levels produced in the presence of a uniform perpendicular magnetic field become broadened by introducing a small periodic component B_m, and the width oscillates with B [3]. At very low magnetic fields, when the period d of the modulation is comparable with the cyclotron radius R_c, so-called commensurability oscillations are expected, and a series of subsingularities (van Hove singularities) at the edges of the broadened Landau levels appear [9], which should produce splittings of the cyclotron resonance (CR). For $R_c \ll d$, new magnetoplasmon (MP) modes arising from the PMMF have been predicted theoretically [4,9,12], and variations in the electron wave function are expected to change the local occupancy of the Landau levels, producing a modulation in the local electron density [4,11]. In the presence of large magnetic field modulations, this effect should produce a transition from a modulated 2DEG to an array of isolated wires [4].

Few of these theoretical predictions have been verified, with experimental data confined to d.c. transport measurements of commensurability oscillations in which the PMMF was produced by evaporating stripes of either superconducting or ferromagnetic materials on top of the 2DEG [6,8,10]. But experimental observations of the optical properties of a 2DEG in a PMMF have yet to be reported.

Here we report the first optical measurements on a 2DEG in the presence of a PMMF. We have investigated the far infrared response of a 2DEG produced using epitaxial regrowth on the canted facets of an etched grating structure so that it has a corrugated profile [13,14]; the component of an externally applied magnetic field perpendicular to the 2DEG is thereby spatially modulated, producing a PMMF without the need for partially obscuring metal stripes. Two active modes are observed, with intensities and frequencies which depend on the amplitude of the magnetic field modulation as well as on the total external magnetic field. The long period of the modulation in our structure ($d \geq 2\ \mu\text{m} \gg R_c$) means that the direct effects on the Landau levels themselves are not observable. Since no plasmon mode is observed at $B = 0$, implying that the corrugated structure does not itself act as a grating coupler, the two modes are interpreted as arising from the PMMF-induced coupling between MPs. We also present calculations of the MP band structure and absorption spectra in the presence of the PMMF, which successfully describe all the experimental data.

The devices were fabricated on a (100) GaAs substrate, and optical lithography was used to produce an array of equally spaced stripes of photoresist with $d = 2\ \mu$m up to $d = 3\ \mu$m. Using an anisotropic buffered hydrofluoric etch, $(n11)B$ ($n \sim 5$) facets were exposed after a vertical etch of 95 nm. After hydrogen radical surface cleaning [15], a superlattice structure was regrown using molecular beam epitaxy on top of the patterned surface. 3 nm of GaAs were grown first, followed by 20 multilayers of 1 nm AlAs and 1 nm GaAs. The 2DEG quantum well (QW) was then realized by growing 7 nm AlGaAs, 15 nm GaAs, 20 nm AlGaAs, a Si-doped (2×10^{18} cm^{-3}) AlGaAs layer 40 nm thick, and finally a 100 nm GaAs capping layer. Since both $(n11)B$, $n \geq 3$, and (100) planes

are known to support electron gases [13,16], the 2DEG produced after the epitaxial regrowth should be continuous and periodically corrugated in one direction. Figure 1(a) shows an atomic force microscope (AFM) image of the 2 μm period sample. The inclination of the facets to the substrate was measured as $\alpha \simeq 13°$ after the epitaxial regrowth.

In a 2DEG, the orbital motion is determined by the perpendicular component of the magnetic field. The 2DEG shown in Fig. 1(a) experiences, in the presence of a uniform applied magnetic field B, a perpendicular component $B_\perp$ which is periodically modulated in the direction perpendicular to the originally etched stripes. The strength of this modulation can be tuned by changing the angle β between B and the perpendicular to the sample substrate, as shown in Fig. 1(b).

A squared mesa without any uncorrugated regions was etched, and Ohmic contacts made to the 2DEG to measure the resistance both along and perpendicular to the corrugation for several devices characterized by a different period. A flat QW was also grown as a reference sample. Similar behavior was observed in all samples, and we concentrate here on the data for the sample with $d = 2$ μm, which had after regrowth a top (100) facet ~800 nm wide, a bottom (100) facet ~600 nm wide, and two lateral facets ~400 nm wide, as shown in the AFM image in Fig. 1(a). Magnetoresistance measurements on the corrugated samples (at $T = 3.3$ K, with B up to 8 T, and a bias current of 100 nA) verified the continuity of the 2DEG, and that the resistances along and perpendicular to the corrugation were similar. Commensurability oscillations were not observed because of the large period of the sample. The optical measurements were performed at $T = 3.3$ K with a Fourier transform infrared (FTIR) spectrometer using unpolarized radiation. The devices were wedged at 5° to avoid interference effects. The relative transmission $[-\Delta T/T = 1 - T(B)/T(B = 0)]$, or absorption, were recorded at various B and β to vary the magnitude of the field modulation.

The uncorrugated reference sample shows a single CR absorption peak at $\omega_c = eB_\perp/m^* = eB\cos\beta/m^*$, corresponding to $m^* = 0.071 m_e$, e being the electronic charge and m_e the free electron mass, as expected for transitions between adjacent Landau levels and in accord with Kohn's theorem [17]. Changing β produced only the expected reduction in ω_c arising from the reduction in $B_\perp$, confirming that introducing an in-plane component of B does not affect the CR. (Another small peak at 112 cm^{-1} was independent of β, and therefore not due to absorption from the 2DEG.)

Figure 2(a) shows absorption spectra for the $d = 2$ μm corrugated sample at $B = 8$ T and various β. For this sample, SdH measurements gave a carrier density of $N_s = 4.5 \times 10^{11}$ cm^{-2} after illumination with band-gap light. A single peak at ~100 cm^{-1} is observed for $\beta = 0°$; this shifts down in energy with increasing β, and a second peak evolves on its high energy shoulder. The intensity of

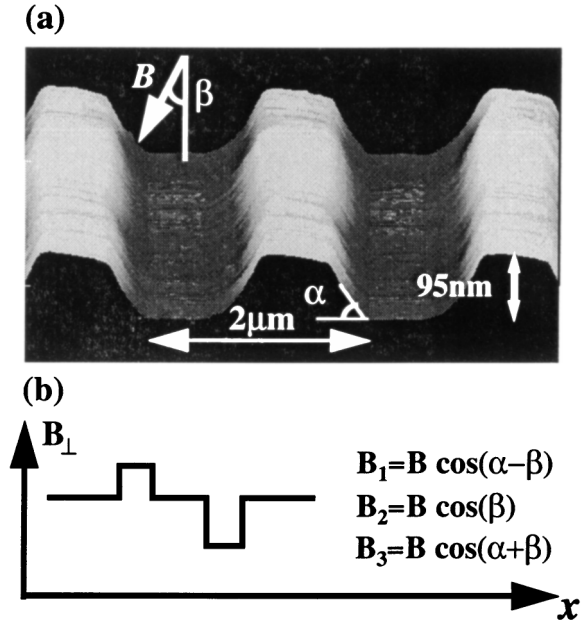

FIG. 1. (a) AFM image of the $d = 2$ μm sample taken after the epitaxial regrowth. (b) Component of the external magnetic field B perpendicular to the corrugated 2DEG.

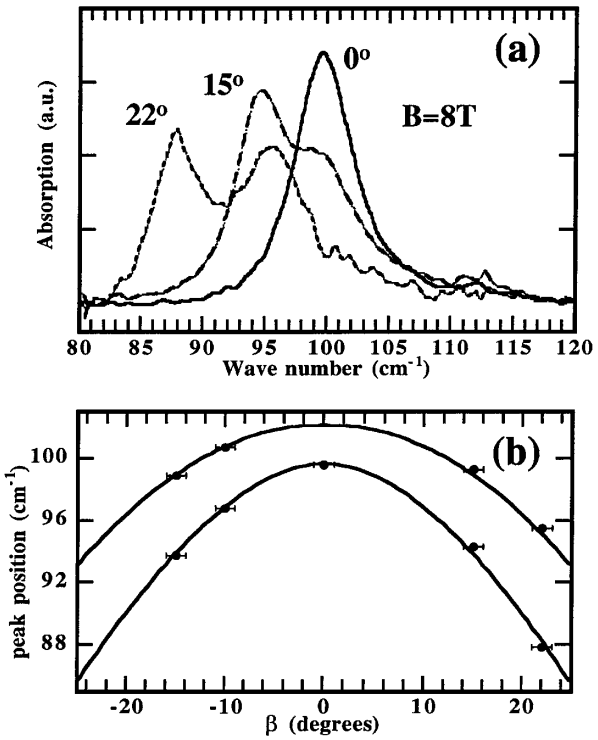

FIG. 2. (a) Absorption spectra measured at various β. Continuous line, dashed line, and dotted line show spectra measured, respectively, at $\beta = 0°$, 15°, and 22°. (b) Peak positions vs β; dots are experimental points, while continuous lines are the lowest two modes obtained from Eq. (3) for various β.

the high energy peak increases with β, as does the energy separation between the two observed peaks. $\beta = 22°$ is the maximum angle usable without strongly affecting the quality of the absorption spectra.

Figure 3(a) shows spectra for $\beta = 22°$ at various B. It is clear that the two modes are coupled: at $B = 8$ T the intensities of the two peaks are similar, while with decreasing B the intensity of the low frequency peak increases and that of the high frequency peak decreases, until, at $B < 4$ T, only the lower frequency peak is observed. The separation between the two peaks also increases with increasing B, as shown by the data points in the dispersion diagram in Fig. 3(c). The splittings we observe are very robust: increasing the temperature up to $T = 80$ K produces only a decrease in the intensity and an increase of the linewidth of the two peaks.

This coupling clearly shows that the two peaks are not simply different CR modes on the different facets, and that something more intriguing is going on. In particular, the high energy branch in Fig. 3(c) clearly shows nonlinear behavior and does not pass through the origin, indicating

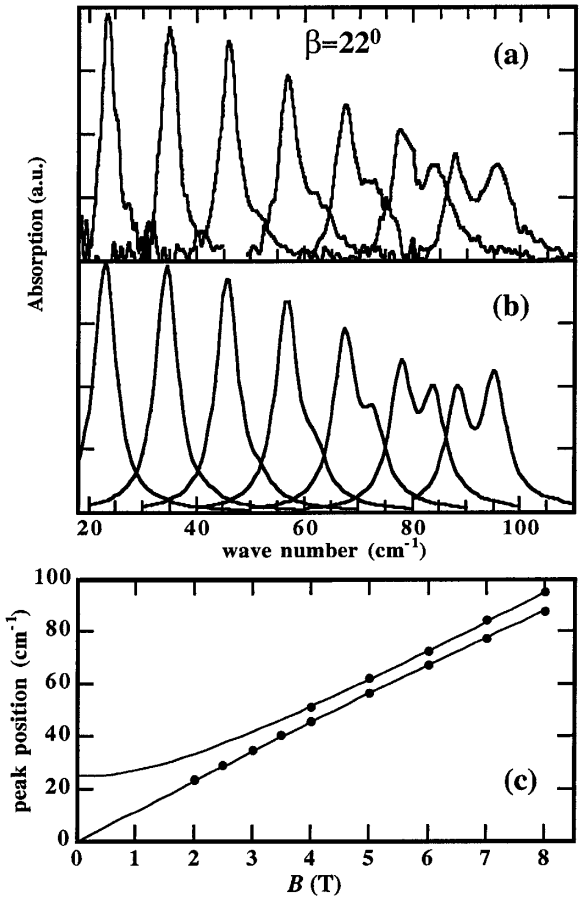

FIG. 3. (a) Absorption spectra measured at $\beta = 22°$ and various B. (b) Absorption spectra $\mathcal{A}(\omega)$ calculated from Eq. (4). (c) The data points mark the peak positions measured at various B for $\beta = 22°$. Continuous lines are the lowest two modes obtained from Eq. (3).

that it might be related to a magnetoplasmon (MP) mode. A MP mode, normally optically inactive, could be excited because of the periodicity of the PMMF, and its intensity, determined by its degree of coupling to the CR mode, should increase with the strength of the PMMF.

To model the optical response of the MP, and to calculate its band structure in the corrugated samples in a uniform applied field B, we treat the 2DEG as if it were *planar* rather than corrugated, and the external magnetic field as if it were, in fact, *periodically modulated* as in Fig. 1(b). We neglect the in-plane component of B which we know from the reference sample does not affect the infrared spectra, and also any contribution from the edges between the (100) and the lateral facets where $B_\perp$ changes. We also ignore any changes the corrugation may have on the electron-electron interactions in the 2DEG since the facet angles are relatively small ($\alpha \approx 13°$), and assume that N_s for the "flat" 2DEG is uniform with a value given by the SdH measurements. In this scenario we can define a local cyclotron frequency $\omega_c(x) = eB_\perp(x)/m^*$, and we calculate the MP band structure by assuming that the PMMF couples together MP modes with wave vectors q differing by reciprocal lattice vectors $G_n = 2\pi n/d, n = 0, \pm 1, \pm 2, \ldots$. In the absence of such coupling the MP dispersion with q is given by

$$\omega_{\mathrm{MP}}(q) = \sqrt{\omega_c^2 + \omega_p^2(q)} = \sqrt{\omega_c^2 + \frac{N_s e^2 q}{2\epsilon\epsilon_0 m^*}}, \quad (1)$$

where ω_p is the 2DEG plasma frequency in the absence of B, and $\epsilon = 12.5$ is the average dielectric constant of the system surrounding the 2DEG. The coupling terms between modes with different q can be determined by considering the spatial Fourier components of the PMMF, i.e.,

$$\Delta_{ij} = \frac{1}{d}\int_0^d e^{i(G_i - G_j)x}\,\omega_{\mathrm{mod}}(x)\,dx\,, \quad (2)$$

where $\omega_{\mathrm{mod}}(x) = \omega_c(x) - \omega_{\mathrm{avg}}$, $\omega_{\mathrm{avg}} = eB_{\mathrm{avg}}/m^*$, and B_{avg} is the average perpendicular magnetic field. The Hamiltonian $\hat{H}$ of the system, considering all the MP modes coupled together, can be written as

$$\hat{H}_{ij} = \omega_{\mathrm{MP}}(q + G_i)\delta_{ij} + \Delta_{ij}\,. \quad (3)$$

The energy dispersion of the coupled modes are then determined by calculating the eigenvalues of $\hat{H}$.

Figure 4 shows the MP band structure calculated for $\beta = 22°$, with energy gaps at edges of the Brillouin zone; the dots show the two modes at the zone center which are observed in the infrared spectra. Continuous lines in Fig. 3(c) show the ω vs B dispersion for these lowest two modes, calculated by including the coupling terms up to $|n| = 4$ in Eq. (3); inclusion of higher order modes produces a negligible effect. We show only the B dispersion of the lowest two modes because the intensities of the higher modes are very small; their only effect is to add a tail on the high frequency side of the main

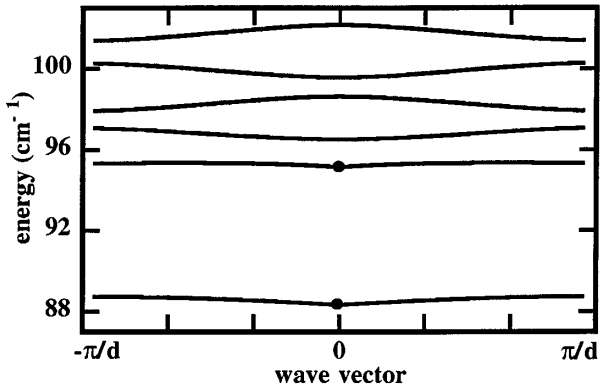

FIG. 4. Magnetoplasmon band structure for $B = 8$ T and $\beta = 22°$. Dots indicate the two main optically active modes observed experimentally.

absorption peaks [see $\beta = 22°$ in Fig. 2(a)], without affecting their positions. The effect of the strength of the PMMF on the two peaks can also be determined from Eq. (3) by varying β. Figure 2(b) shows experimentally observed peak positions vs β (data points), and the corresponding mode energies calculated from Eq. (3) for various β (continuous lines).

It is important to note that the continuous lines in Figs. 2(b) and 3(c) are calculated without any fitting parameters; *all* the physical quantities $[N_s, d, B_{\mathrm{mod}}(x), m^*]$ used in the calculation have been determined experimentally, and the agreement between the calculated curves and the experimental data is excellent. The energy dispersions calculated for various β for samples with different periods d are also in excellent agreement with the corresponding experimental data.

The infrared absorption spectra can also be calculated from the response of $\hat{H}$ in the presence of an external perturbation, the infrared electromagnetic field. We should again note that the MP is not observed at $B = 0$, which implies that direct coupling with the diffracted light produced by the surface modulation is negligible, and that the MP mode is excited only via PMMF-induced coupling to the CR-like mode. The absorption spectra can therefore be determined by solving

$$[\hat{H} - \hat{I}(\omega + i\gamma)]\Psi = \Theta\,, \tag{4}$$

where Ψ is the response of the driven system to Θ, the external driving force (the FIR electromagnetic field), and $\hat{I}$ is the identity matrix. The elements θ_i of Θ are given by the different spatial Fourier components of the external electromagnetic field, and γ represents the energy broadening present in the real spectra. Since the wavelength λ of the infrared radiation is much larger than d, and any diffracted fields resulting from the corrugation are negligible, we take $\theta_i \approx \delta_{i0}$, i.e., only the $G = 0$ MP mode is directly driven. The absorption $\mathcal{A}(\omega)$ can be then calculated from the imaginary part of ψ_0, i.e., $\mathcal{A}(\omega) = \Im\{\psi_0\}$.

Figure 3(a) shows the infrared absorption measured at $\beta = 22°$ and various B, while Fig. 3(b) shows the corresponding spectra calculated as described above; here, we have introduced the broadening parameter $\gamma = 2.5\ \mathrm{cm}^{-1}$, which was determined from the linewidth of the spectra at $B = 8$ T and $\beta = 0°$. This value of γ is also very similar to that measured for the uncorrugated sample under the same experimental conditions. The agreement, in terms of peak positions and relative intensities, is again excellent.

In conclusion, we have reported the first optical measurements on a 2DEG in the presence on a periodically modulated magnetic field. The absorption spectra show two modes, with relative intensities and separation depending on the strength of the magnetic field modulation, as well as on the total external magnetic field. The two modes have been interpreted as arising from coupling between magnetoplasmon modes due to the magnetic field modulation. Magnetoplasmon band structure and absorption spectra calculations have been used to model all the experimental results without fitting parameters, and the agreement between the experimental data and the theory is excellent.

[1] R. W. Winkler, J. P. Kotthaus, and K. Ploog, Phys. Rev. Lett. **62**, 1177 (1989).
[2] P. Vasilopoulos and F. M. Peeters, Phys. Scr. **T39**, 177 (1991).
[3] F. M. Peeters and P. Vasilopoulos, Phys. Rev. B **47**, 1466 (1993).
[4] X. Wu and S. E. Ulloa, Phys. Rev. B **47**, 7182 (1993).
[5] I. S. Ibrahim and F. M. Peeters, Phys. Rev. B **52**, 17 321 (1995).
[6] S. Izawa, S. Katsumoto, A. Endo, and Y. Iye, Jpn. J. Appl. Phys. **34**, 4306 (1995).
[7] M. Leadbeater *et al.*, Phys. Rev. B **52**, 8629 (1995).
[8] P. D. Ye *et al.*, Phys. Rev. Lett. **74**, 3013 (1995).
[9] S. M. Stewart and C. Zhang, J. Phys. C **8**, 6019 (1996).
[10] Q. W. Shi and K. Y. Szeto, Phys. Rev. B **55**, 4558 (1997).
[11] U. J. Gossmann, A. Manolescu, and R. R. Gerhardts, Phys. Rev. B **57**, 1680 (1998).
[12] A. Manolescu and V. Gudmundsson, Superlattices Microstruct. **23**, 1169 (1998).
[13] S. Cina *et al.*, Physica (Amsterdam) **249B–251B**, 286 (1998).
[14] S. Cina *et al.*, Jpn. J. Appl. Phys. **37**, 1570 (1998).
[15] T. M. Burke *et al.*, J. Cryst. Growth **175/176**, 416 (1997).
[16] W. I. Wang, E. E. Mendez, T. S. Kuan, and L. Esaki, Appl. Phys. Lett. **47**, 826 (1985).
[17] W. Kohn, Phys. Rev. **123**, 1242 (1961).